

## Estimating the Landslides magnitudes along the Na'ur–Dead Sea Highway- Jordan by Using Geomatics Techniques

<sup>1</sup>Akawwi Emad, <sup>2</sup>AIRzouq Rami, <sup>3</sup>Nidal Hadadin, <sup>4</sup>Qtishat Khaldon, <sup>5</sup>Alabsi Islam, <sup>6</sup>Al-Qara Karam

<sup>1</sup>Surveying and Geomatics Department, Faculty of Engineer, Al-Balqa Applied University- Salt 19117 JORDAN.

<sup>2</sup>Computer engineer, Al-Balqa Applied University, Salt 19117, JORDAN  
The Hashemite University-Zarka.

<sup>4</sup>KADDB Company, JORDAN.

<sup>5</sup>Al-Balqa Applied University-Salt, JORDAN.

<sup>6</sup>Al-Balqa Applied University, JORDAN.

---

**Abstract:** Landslides can be triggered by external mechanisms including undercutting of a slope by stream erosion, wave action, glaciers, or human activities as building intense or prolonged rainfall, rapid snow melt, or sharp fluctuations in ground-water levels. Shocks or vibrations caused by earthquakes or construction activity. Jordan is one of the countries of the world suffering from the landslides at different cities due to the swelling of the clay materials in some subsurface geological formations as Fuhais-Hummar-shu'yeb formation from the Cenomanian age. The locations of the landslides and deformations along Na'ur – Dead Sea road, the water surfaces flow directions and the slope of the geological layers of the study area, the drainage pattern of the eastern region of the Dead Sea, the locations and magnitudes of the recent landslides were determined in this study. The main landslides were found at the coordinates E 768598.508 and N 3530685.801. The magnitude of the deformation at this point is 7.8 cm. The reason of the landslide of the study area was determined. The main reason of the landslides is the heavy rain that happened in the last three days before the last measurements. These precipitations infiltrate into the subsurface layer reaching the clayey layers. These clayey layers get swelling due to absorb the water. The main type of drainage pattern in the study area was determined by using the aerial photos and satellite images by using the ARC-Hydro extension of GIS. The main type of the drainages is high-density dendritic drainage pattern. As well the satellite images were used to determine the surface water flow direction by using the GIS. The surface-water flow direction was found toward the Na'ur-Dead Sea highway. As well the slope aspect of the study area was carried out by using the GIS software. The slope of the layers was determined toward the southwest direction.

**Key words:** rock deformations, Dead Sea, Na'ur, Drainage pattern, GIS, Arc-Hydro.

---

### INTRODUCTION

Landslides are naturally-occurring geologic processes that commonly cause different types of damages to people and construction in addition to landscapes. They defined as “abrupt, short-lived geomorphic events that constitute the rapid motion end of the mass-movement spectrum” (Coates, D., 1977). A landslides inventory, or landslide map, is representation of the spatial distribution of deposition and erosion areas of gravity-induced mass movements (Guzzetti *et al.* 1999). The slope movement can be predicted by knowing the spatial distribution of relict and recent landslides (Carrera *et al.* 1995). Pohl and Van Genderen (1998) use image fusion techniques in order to obtain a new hybrid image with the best characteristics of the two original images in different years.

The assessment of landslide hazard and risk has recently become a topic of interest for geoscientists and local administrations (Van western *et al.*, 2000, Krejci *et al.* 2002; Demoulin and chung, 2007; Nefesiolgue *et al.* 2008).

The landslide hazard mapping techniques divided into two groups. The first one direct hazard mapping, the degree of hazard is determined by the mapping geomorphologist, based on his experience and knowledge of the terrain condition; and the second is indirect hazard mapping, in which either statistical models or deterministic models are used to predict landslide prone areas (Van Westen *et al.* 1999). By the increasing availability of high-resolution spatial data sets, GIS, remote sensing, and computers with large and fast processing capacity, it is becoming possible to partially automate the landslides hazard and susceptibility mapping process and thus minimize fieldwork (Ayalew and Yamagishi, 2005, Fall *et al.* 2006; Zolfaghari and Heath, 2008; Yalcin, 2008).

---

**Corresponding Author:** Akawwi Emad, Surveying and Geomatics Department, Faculty of Engineer, Al-Balqa Applied University- Salt 19117 JORDAN.  
E-mail: ejeakawwi@hotmail.com

Many scientists as (Ohlmacher and Davis 2003, Gorsevski *et al.*, 2006; Castellanos Abella and Van Westen 2008) have used the GIS and statistical models.

Rainfall-induced slope failure is common form of landslide (Brand *et al.* 1984, Crosta 1998, Dai *et al.*, 2003, Tsai and Yang, 2006).

Landslides cause property damage, injury and death, and adversely affect a variety of resources.

The negative economic effects of landslides include the cost to repair structures, loss of property value, distribution of transportation routes, medical costs in the event of injury and indirect costs.

Water availability, quantity and quality also can be affected by landslides

Most of the slides occurred during or shortly after the winter season. Few slides occurred shortly after excavation in summer. However, all the slides were associated with the presence of wet or saturated layers or perched water (Al-Hamoud *et al.* 1996). As well, the slides occurred in the rugged areas of old landslides with moderate to steep topography where the shear strength approximates the residual one.

Many factors contribute to the instability of slopes, but the main controlling factors are the nature of underlying bedrock and soil, the Configuration of the slope, and ground water conditions.

Three distinct physical events occur during a landslide: the initial slope failure, the subsequent transport, and the final deposition of the landslide material.

slope stability problems of this highway are attributed to the presence of weak friable of some of the interbedded sediments and their sensitivity to fluctuations in water content. The study area incorporates good exposure of sedimentary rocks including limestone, marl, sandstone, chalk and chert.

More than 50% of landslides are associated with plastic marls and about 20% with shales. The rest of landslides occurred mainly in fill materials placed over metastable colluvial deposits, and in saturated superficial (Al-Hamoud *et al.* 1996). Deposits composed of clays, silty clays, and sandy silts. Most of the landslides occurred in the marls of the Na'ur and Fuheis Formations, A<sub>1</sub>-A<sub>2</sub> and A<sub>3</sub> of the Ajlun Group (Cenomanian-Turonian age), and about 28% of the slides occurred in the weak recent superficial deposits. About 20% of the slides occurred in the clays tones and shales of the Kurnub Sandstones (Lower Cretaceous). Most of the major landslides in Jordan are linked with the A<sub>1</sub>-A<sub>2</sub> (Na'ur Formation) and A<sub>3</sub> (Fuheis Formation) of the Ajlun group, and fewer are linked with either the silty shale and claystone intercalations within the Kurnub sandstone formation or the recent deposits composed of colluviums, silty clays, and clayey silty sands (Al Homoud *et al.* 1999)

It is interesting to note that the marl and shale which constitute more than 70% of the sliding materials are moderately to highly plastic. Such materials generally have moderate to high swelling potential.

Landslides can be triggered by gradual processes such as weathering, or by external mechanisms including:

- Undercutting of a slope by stream erosion, wave action, glaciers, or human activities as building.
- Intense or prolonged rainfall, rapid snow melt, or sharp fluctuations in ground-water levels.
- Shocks or vibrations caused by earthquakes or construction activity.
- Loading in upper slopes or combinations of these and other factors.

The aims of the study are to determine the locations of the landslides and deformations along Na'ur – Dead Sea road, to determine the water surfaces flow directions and the slope of the geological layers of the study area in addition to estimating the magnitudes of the recent landslides.

#### ***Regional Background and Geological Setting:***

The study area covers the route of Na'ur-Dead sea highway. It located at the following coordinates (E 764240.593, N 3535295.699 and E 775482.681, N 3535307.474 and E 775477.095, N 3523921.962 and E 764231.855, N 3523917.636). Figure 1 shows the location map of the study area.

Climate in area is semi arid: temperatures vary between -2 C in January and 38 C in august. Annual precipitation is ca. 650 mm/year and evaporation from 300 to 400 mm/year. Snow fall two to three times a year with a 40-50 cm between January and March. After melting causing high water, stand in both soil and streams.

Structurally the Na'ur – Dead Sea highway pass through the lower part of the Ajlun group (marl, limestone, and limestone –marl) formations of the middle and upper cretaceous. The upper most part of the Ajlun group is frequently overlain by surface cover and weathering products of the quaternary period. The Kurnub sandstone of the lower cretaceous is also encountered, though to a lesser degree.

Kurnub sandstone is uncomformably overlain by a thick sequence of carbonate rocks represented by the Ajlun Group (Cenomanian-Turonian). The Early Cretaceous Kurnub Group of Jordan consists of three regressive-transgressive (fluvial-marine) depositional sequences in northern Jordan, recorded here for the first time, whereas continental clastics dominated central and southern Jordan. Deposition of the Kurnub Group started in the late Neocomian above a regional angular unconformity by basal conglomerate and sandstone facies association of an alluvial braidplain origin (Abed 1978 and Abed 1982).

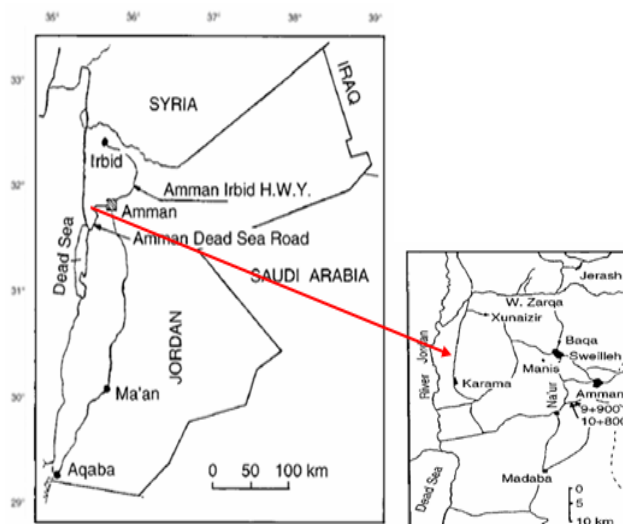


**Fig. 1:** The location of the study area.

Nau'r limestone formation (Cenomanian) is one of sediments outcropping in the study area. The formation is up to 180 m thick. The basal part (juhra Members) is 33 m thick and consists of fine to grained sandstone Interbedded with siltstone, mudstone, and marl. The upper part of the formation consists of Shelly limestone, marl, dolomitic limestone and dolomite with chert nodules at the top.

The Fuhays formation is up to 55 m thick and consists of grey-green marl, calcareous siltstone, thinly bedded nodular limestone and secondary gypsum. The Shu'ayb formation is up to 48 m thick in the study area and consists of nodular limestone, marl, marly limestone, dolomite limestone coquina, fossiliferous limestone and nodular marly limestone.

The Wade As-Sir limestone formation covers broad areas of the study area. The formation is 90m thick and consists of bedded massive Limestone, hard buff dolomite limestone with subsidiary marls and chart nodules common In the middle and the upper parts.

Marls and marly limestone deposits cover most of northern Jordan, where Amman city and its suburbs are located. These deposits serve as foundations for most buildings and roads as well as fill material for structural back filling, especially road bases and sub-bases. Figure 2 shows the geological layers in the study area.

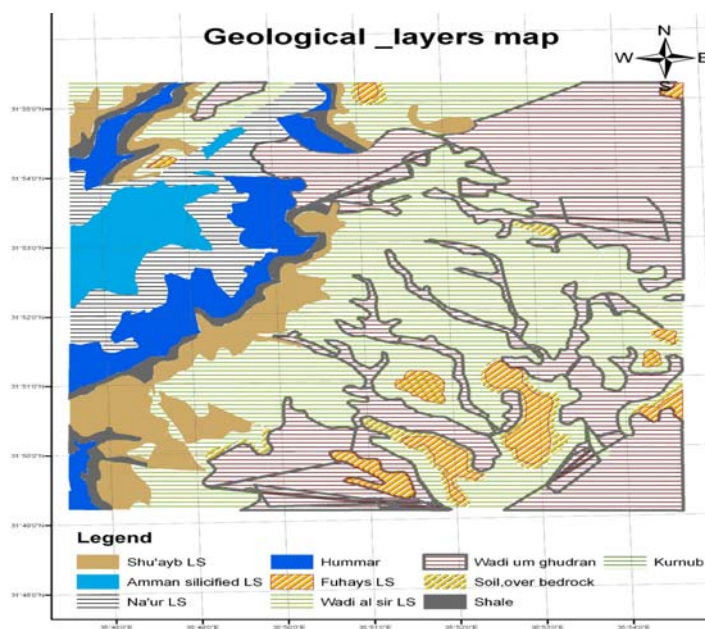


**Fig. 2:** The geological layers in the study area.

## MATERIAL AND METHODS

There are many approaches to assessing slope stability and landslides hazards.

The most widely used include:

- a- Field inspection using a check list to identify sites susceptible to landslides.
- b- Projection of future patterns of instability from analysis of landslides inventories.
- c- Multivariate analysis of factors characterizing observed sites of slopes instability.
- d- Stability ranking based on criteria such as slope, lithology, land form, or structure and
- e- Failure probability analysis based on slope stability models with stochastic hydrologic simulations.

Recently, growing availability of GIS systems and popularity of data inform of Digital Elevation Models (DEM) along with tools for their processing and analyzing, collecting terrain topography data that are essential for slope stability analysis purpose, has become considerably easier and less time-consuming.

This study attempted to use integrated Remote sensing GPS techniques and Geographic Information System (GIS) techniques to identify the areas prone landslides and deformations. As well, the GIS (Arc-hydro extension) were used for determining the watershed and the drainage pattern system for the study area.

Topographic maps for Amman with scale 1:50,000 was used for issuing the digital elevation model of the area. The geological maps for Amman with scale 1:50,000 was used for determining the geological features of the study area.

The colored aerial photographs for Amman with scale 1:25,000 was taken in 2000, and black and white aerial photos for Amman in 1993 with a scale of 1: 30000 were used to determine the development of the rock fall and the landscape along the highway.

The satellite spot images with 15-meter resolution were taken in 2007, Landsat images with 30 meter resolution was taken in 2002 and the geological subset for Amman issued in 2007 were used as base map for the Arc-hydro extension of the GIS for creating the drainage pattern system of the study area.

In some cases, Landsat TM scenes are much larger than a project study area. In these instances it is beneficial to reduce the size of the image file to include only the area of interest. This not only eliminates the extraneous data in the file, but it speeds up processing due to the smaller amount of data to process. This is important when utilizing multiband data such as Landsat TM imagery. This reduction of data is known as subsetting. This process cuts out the preferred study area from the image scene into a smaller more manageable file.

In order to integrate various types of images and spatial data in a GIS environment, the digital image data must first be in the same coordinate system and geo-referenced. After geo-referencing the pixels in the new image keep their original row and column values. All data used in this study were geo-referenced in the Universal Transverse Mercator (UTM) coordinate system as the map projection and World Geodetic System (WGS) 1984 datum. In order to have comparable resolution, the majority of images were resampled to 2.5 m. In some case where greater detailed analysis was needed, images were resampled to 1.5 m resolution. The data was then rectified so that it could be combined with other data sets, which had a different datum. ENVI 4.3 were used to geo-reference and rectify the raw digital image data, and to apply various enhancement methods.

The Ground control points (GCP's) were collected from 1:50000 topographic maps for Amman and from Aerial photographs that covered the study area, GCP's are landmarks, which are identifiable on both images and maps. We have selected landmarks for image registrations such as crossroads, bridges and railroads crossing. However, because of the insufficient correspondence of map road net, and the actually existing road net and the topographic base maps not being up to date, it has been difficult to cover the map with well-distributed and precise GCP's. Figure 3 shows the locations of the GCP's.

Since our study depends on deformations and land slides along Na'ur –Dead Sea highway, the field surveying is a very important step to get the coordinates of the GCP's that we've fixed along the highway and the surrounding area using high resolution GPS. As well the total stations were used in order to determine the coordinate (X, Y) positions for all the control points. Many field trips in a different time have been done.

The first trip was on first of MAY 2008, the second was on 26 AUG 2008 and the last one was on 6 MAR 2009 after a heavy rain days.

Change Detection Analysis encompasses a broad range of methods used to identify, describe, and quantify differences between images of the same scene at different times or under different conditions. The ENVI's tools (such as Band Math or Principal Components Analysis) independently, or in combination, as part of a change detection analysis were used.

In addition, the routines found under the ENVI main menu option Basic Tools Change Detection offer a straightforward approach to measuring changes between a pair of images that represent an initial state and final state.

The compute difference Map was used to produce an ENVI classification image characterizing the differences between any pair of initial state and final state images.

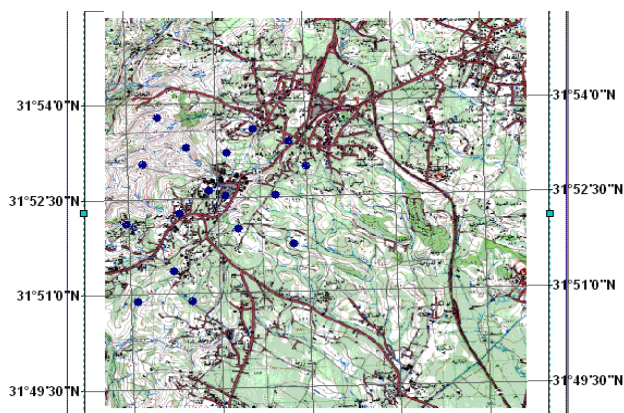


**Fig. 3:** The locations of GCP's.

The change detection method was applied in this study on both (1993) aerial photographs and (2000) for the studied area so that we can notice the differences that happens on the area and specially the highway.

This technique is an extremely popular and powerful use of remotely sensed data. Assessing the accuracy of a change detection analysis has all the issues, complications, and difficulties of a single date assessment plus many additional, unique problems.

Geographic information systems GIS have been evolving from basic spatial data storage\_ retrieval and display systems to more powerful spatial modeling systems. This transition is mainly due to more robust query capabilities the creation of spatial query languages that empower the end user to design and create spatial models will advance this development even further.

The paper maps were converted into a digital format maps. Then these digital maps were registered and rectified by using the Arc-GIS (Arc Map). Then layers for all features were created as a shape files depending on the type of the features.

A triangulated irregular network (TIN) is a data model commonly used to represent terrain heights. Typically the x, y, and z locations for measured points are entered into the TIN data model. These points are distributed in space, and the points may be connected in such a manner that the smallest triangle formed from any three points may be constructed. The TIN forms a connected network of triangles. Triangles are created such that the lines from one triangle do not cross the lines of another. Triangle is drawn only if the corresponding convergent circle contains no other sampling points. Each triangle defines a terrain surface, or facet, assumed to be of uniform slope and aspect over the triangle.

The TIN model typically uses some form of indexing to connect neighboring points. Each edge of a triangle connects to two points, which in turn each connect to other edges. These connections continue recursively until the entire network is spanned. Thus, the TIN is a rather more complicated data model than the simple raster grid when the objective is terrain representation.

A triangulated irregular network (TIN) is an example of such a data model. This model is the most often used to represent surfaces, such as elevations, through a combination of point, line, and area features. Many consider this a special, admittedly well-developed, type of vector data model.

## RESULTS AND DISCUSSIONS

By applying change detection in many places we found that there is a clearly change happened to the area in that period. The stability of the landslide area has been assessed using limit equilibrium analysis and classifications. The geological conditions and other reasons were determined by analyzing and interpretation processing and enhancements. There are a strong relationship between the rocks formation and landslides in the area. The results of both remote sensing and GIS were used in describing the factors that effect on the landslides and deformations along the Na'ur – Dead Sea highway. The results from applying enhancements, processing and finally classifications of satellite images showed that there are some changes between the aerial photos that taken in 1993 and the aerial photos that taken in 2000. The landslides and deformations increased in 2000. The results of the change detections are shown in figure 4. The areas of high change detection are denoted by a blue color while the areas of no change detections are denoted by red color.

The GPS results that we have got from the field measurements are summarized in the table 1. The GPS results showed that there are no changes in the coordinates in the measurements in the second trip. While the measurements in the third trip showed that significance change in the coordinates at certain locations. These changes in the coordinates are a remarkable of the rock deformations and landslides. These changes are due to

heavy rains in the last ten days before carrying the last measurements. The most changes are at the points ID numbers 8, 3, 6, 11, 10 and 7 at the coordinates E 768598.508 and N 3530685.801, E 768147.039 and N 3530737.889, E 767539.052 and N 3529819.776, E 767402.010 and N 3531101.431, E 767344.671 and N 3529424.625 and E 768871.966 and N 3531282.647 respectively. The magnates of the deformation at these points are 7.8 cm, 6.4 cm, 5.6 cm, 5.5 cm, 5.4 cm and 4.1 cm respectively.

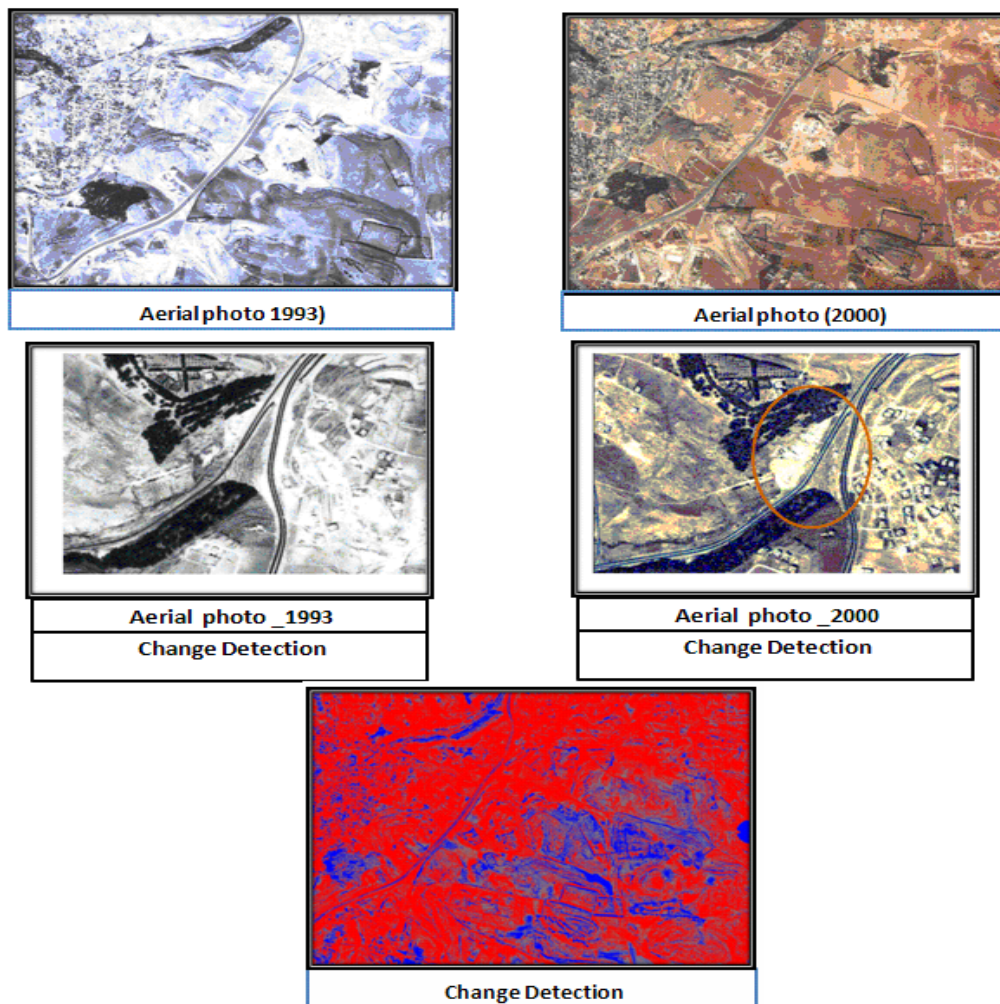


**Fig. 4:** The enhancement shows the change detection of the study area.

The significance changes at these points are due to the high content of clay and marl materials, which, affect significantly of the landslides.

**Table 1:** The reading of the ground control points along the Na'ur- Dead Sea highway.

Point ID	Coordinates of 1 <sup>st</sup> trip		Coordinates of 2 <sup>nd</sup> trip		Coordinates of 3 <sup>rd</sup> trip	
	East	North	East	North	East	North
1	768863.962	3531072.464	768863.964	3531072.466	768863.968	3531072.480
2	768683.058	3531064.579	768683.061	3531064.580	768683.081	3531064.61
3	768147.039	3530737.889	768147.042	3530737.890	768147.054	3530737.953
4	767847.021	3530459.056	767847.023	3530459.060	767847.039	3530459.075
5	768831.1450	3531214.439	768831.148	3531214.440	768831.152	3531214.458
6	767539.052	3529819.776	767539.056	3529819.780	767539.076	3529819.822
7	768871.966	3531282.647	768871.964	3531282.649	768872.005	3531282.688
8	768598.508	3530685.801	768598.510	3530685.802	768598.584	3530685.879
9	769053.827	3531580.205	769053.827	3531580.205	769053.847	3531580.225
10	767344.671	3529424.625	767344.674	3529424.628	767344.694	3529424.679
11	767402.010	3531101.431	767402.013	3531101.431	767402.034	3531101.486
12	768882.640	3530512.416	768882.641	3530512.417	768882.665	3530512.428

The variation in elevations in the studying area causes many slides and rock falls. TIN map is a result from contour lines. By applying 3D analysis, we get TIN, which gives a representation for the surface and the more accuracy in digitizing the contour lines the more accurate TIN that we get. From TIN map (figure 7), we can notice that the highest area is that in light blue color and it lies in the NE direction in our map. The lowest area is that which is in the upper NW direction. Na'ur lies in the marked area, the elevation varies in that area and this causes difference in slopes. Figure 5 shows the big differences of the elevations in the study area.

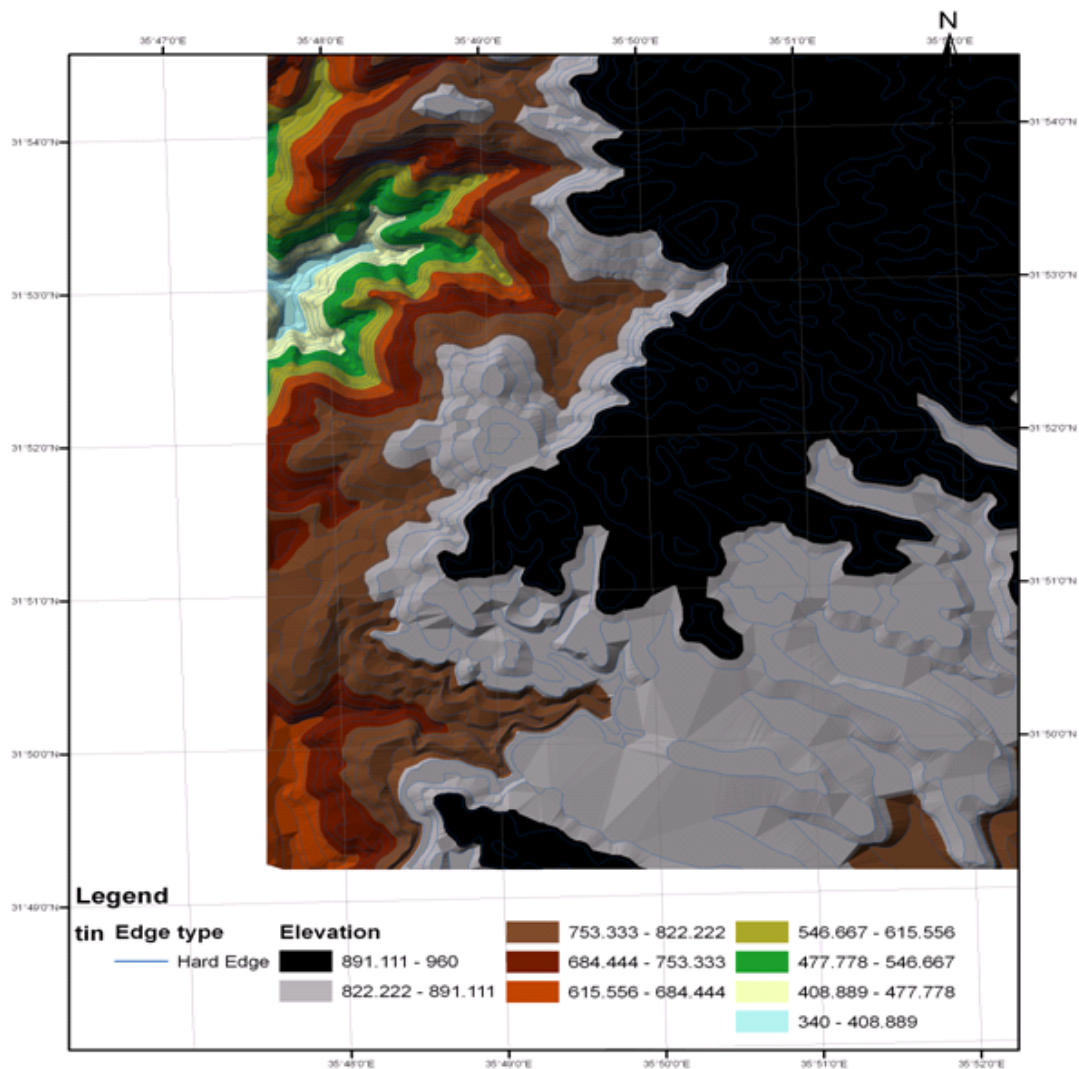


**Fig. 5:** TIN map of the studying area.

The slope has its maximum value at the NW direction of the study area at the following coordinates: (E 765477.022 and N 3534081.311, E 769152.448 and N 3535208.441, E 767143.215 and N 3530732.589, E 764366.226 and N 3529131.736, E 765126.723 and N 3533800.584, E 771985.307 and N 3532902.436, E 772001.637 and N 3527431.898 and E 76800.183 and N 3524378.175). The slopes at these coordinates range between 35 and 68%. These areas are characterized as risky area due to the rock fall. Figure 6 shows the slope map of study area.

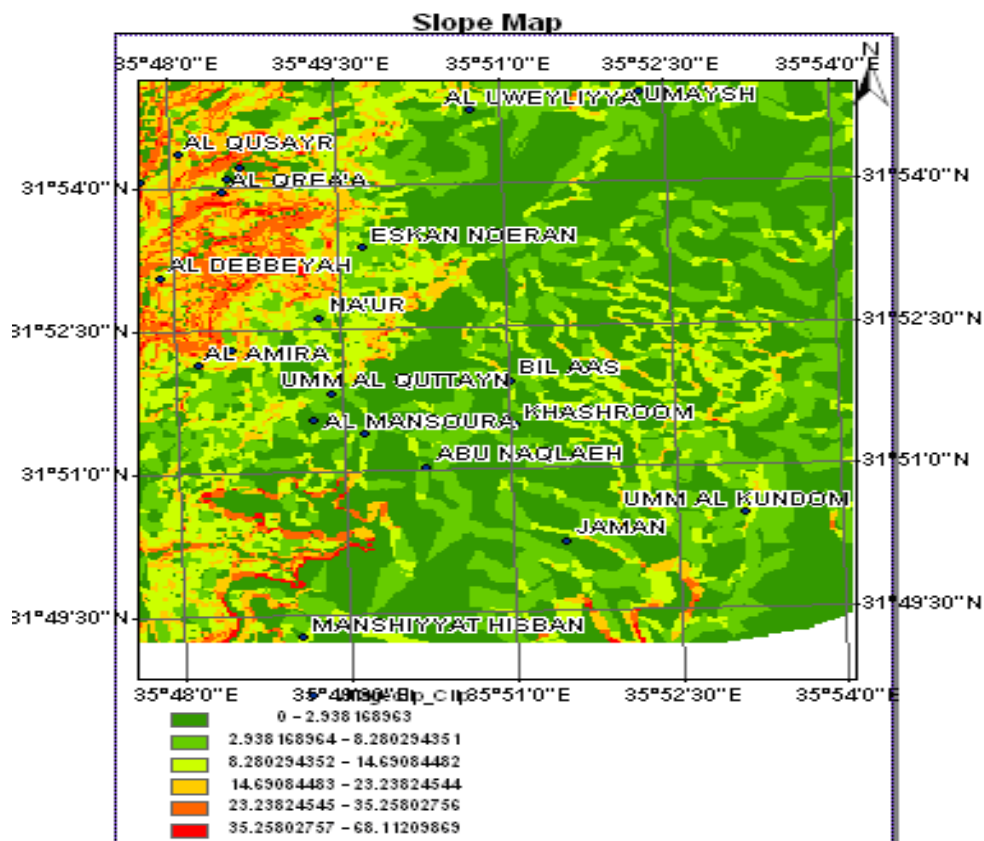


**Fig. 6:** The slope map of the study area.

This figure shows that the highest slopes denoted by the red and orange colors. These highest slope areas located at the NW of the study area. This area also has a heavy wadies network. Geologically the area recognized by a marly limestone and high clay contents. These layers are factors for landslides at the study area.

The water map for Na'ur area (figure 7) shows that the springs are concentrated between (E 764365.7 and N 3530922.3, E 768356.5 and N 3531057.9, E 764395.8 and N 3524913.4 and E 768552.3 N 3525079). These springs affected on the water flow and the drainage pattern in the study area. The shape of the drainage pattern in the study area is mostly dentritic shape and very little drainage is rectangular. The characteristics of the dentritic drainage pattern in the study area are high density and low orientations due to the high contents of the clay materials. The direction of flow is going from southeast (SE) to northwest (NW) towards the Na'ur-Dead Sea road. Because of the slopes are toward this road. Figures 7 and 8 show the drainage system and the spring's locations in the study area.

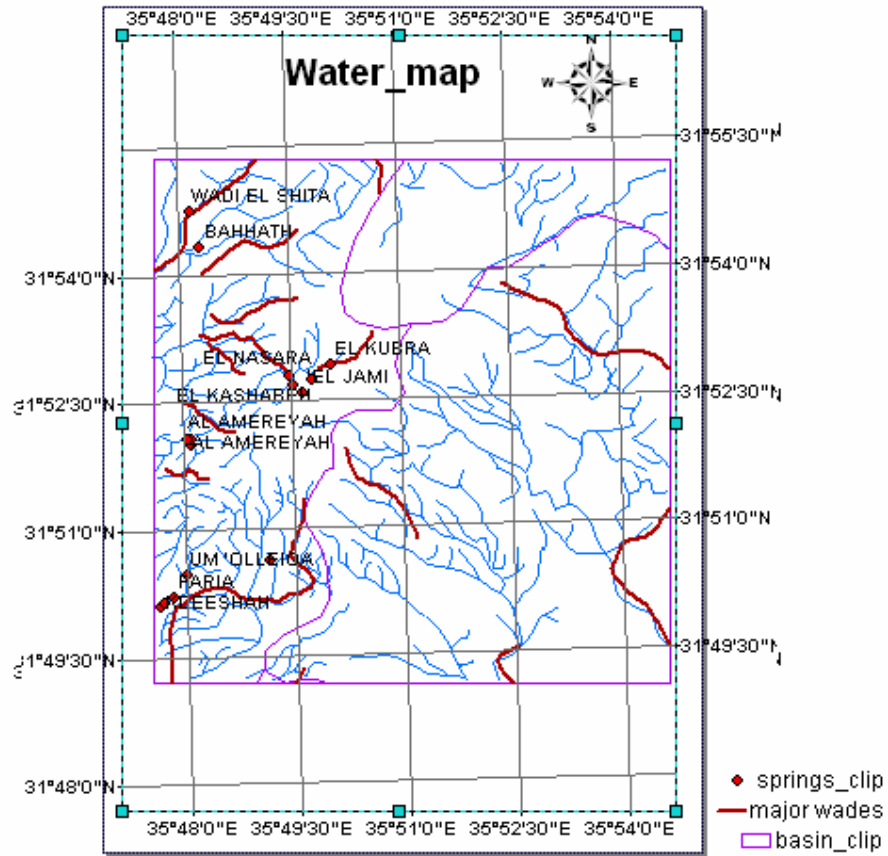


Fig. 7: The drainage pattern system for the study area.

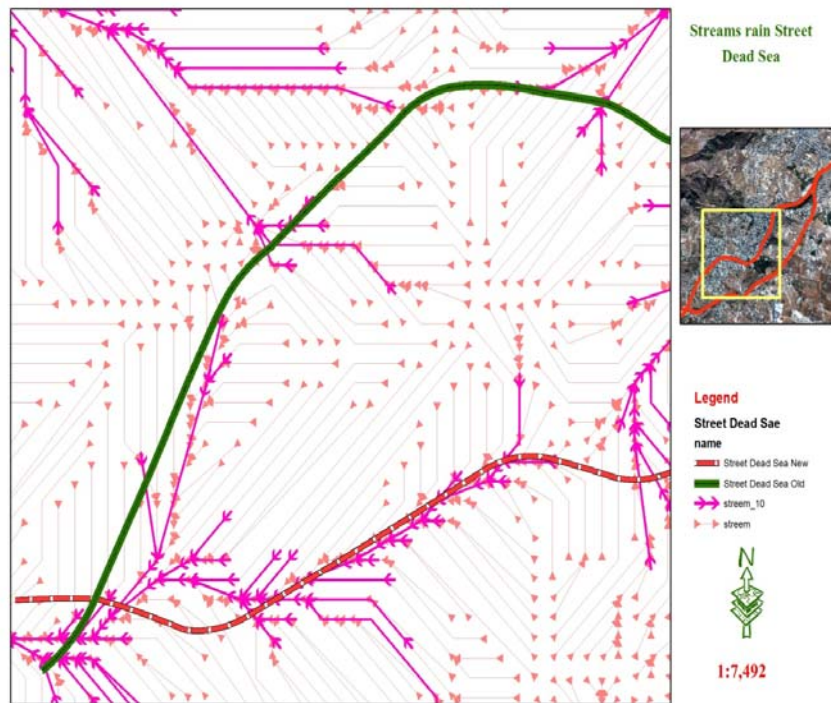


Fig. 8: The Drainage pattern for the area surrounding the Amman-Dead Sea highway.

**Conclusion:**

The Geomatics techniques as the total stations and GPS are very useful for determining the directions and the magnitudes of the rock deformations. The Arc-Hydro extension of the GIS software is very useful for determining the drainage pattern and the surface-water flow directions. The rainfall, the slope and the type of the rocks and soils in the study area are the main factors effect on the landslides and rock formations in the study area. The shape of the drainage pattern in the study area is mostly dentritic shape and very little drainage is rectangular. The characteristics of the dentritic drainage pattern in the study area are high density and low orientations due to the high contents of the clay materials. The direction of flow is going from southeast (SE) to northwest (NW) towards the Na'ur-Dead Sea road. The maximum rock deformation in the study area is the area surrounding the coordinate E 768598.508 and N 3530685.801. The maximum rock deformation in this coordinate is 7.5 cm.

**REFERENCES**

- Abed, A.M., 1978. Depositional environments of the Kurnub (Lower Cretaceous) Sandstones. I. A coal horizon at the lowermost Kurnub, North Jordan. *Dirasat*.
- Abed, A.M., 1982. Depositional environments of the Early Cretaceous Kurnub (Hathira) Sandstones, North Jordan. *Sediment. Geol.*, 97: 267-279.
- Al-Homoud, A., G. Prior, A. Awad, 1999. Modeling the Effect of Rainfall on Instabilities of Slopes Along Highways. *Environmental Geology*, 37(4): 317-325.
- Al-Homoud, A.S., H. Houry, Y.A. Al-Omari, 1996. Mineralogical and engineering properties of problematic expansive clayey beds causing landslides. *Bull. Int. Assoc. Eng. Geol.*, 54: 13-31.
- Ayalew, L., H. Yamagishi, 2005. The application of GIS-based logistic regression for landslide susceptibility mapping in the Kakuda-Yahiko Mountains, Central Japan. *Geomorphology*, 65: 15-31.
- Castellanos Abella, E.A., E.A. Van Westen, 2008. Qualitative landslide susceptibility assessment by multicriteria analysis: A case study from San Antonio del Sur.
- Carrara, A., M. Cardinali, F. Guzzetti, P. Reichenbach, 1995. GIS technology in mapping landslide hazard. In: Carrara, A., Guzzetti, F. (Eds), *Geographical information Systems in Assessing Natural Hazards*. Kluwer Academic Publishers, Dordrecht, pp: 135-175.
- Coates, D.R., 1977. Landslides perspectives, In: Coates, D.R., *Landslides, Reviews in engineering Geology*, Vol. 3. Geological Society of America, Boulder, Colorado, pp: 3-28.
- Crosta, G., 198. Regionalization of rainfall thresholds: an aid to landslide hazard evaluation. *Environmental Geology*, 35(2-3): 131-145.
- Dai, F.C., C.F. Lee, S.J. Wang, 2003. Characterization of rainfall-induced landslides. *International Journal of Remote Sensing*, 24(23): 4817-4834.
- Demoulin, A., C.F. Chung, 2007. Mapping landslide susceptibility from small datasets; a case study in the Pays de Herve (E Belgium). *Geomorphology*, 89: 391-404.
- Fall, M., R. Azzam, C. Noubactep, 2006. A multi-method approach to study the stability of natural slopes and landslide susceptibility mapping. *Engineering geology*, 82: 241-263.
- Gorsevski, P.V., P.E. Gessler, J. Boll, W.J. Elliot, R.B. Foltz, 2006. Spatially and temporally distribution modeling of landslide susceptibility. *Geomorphology*, 80: 178-198.
- Guantanamo, Cuba, *Geomorphology*, 94: 453-466.
- Guzzetti, F. A. Carrera, M. Gardinali, P. Reichenbach, 1999. Landslide hazard evaluation: a review of current techniques and their application in a multi Scale study, Central/Italy. *Geomorphology*, 31: 181-216.
- Krejci, O., I. Baron, M. Bil, F. Hubatka, Z. Jurova, K. Kirchner, 2002. Slope movements in the flysch Carpathians of Eastern Czech Republic triggered by extreme rainfalls in 1997: a case study. *Physics and chemistry of the Earth. Parts a/b/c*, 27(36): 1567-1576.
- Nefeslioglu, H.A., T.Y. Duman, S. Durma, 2008. Landslide susceptibility mapping for a part of tectonic Kelkit Valley (Eastern Black sea region of Turkey). *Geomorphology*, 94: 401-418.
- Ohlmacher, G.C., J.C. Davis, 2003. Using multiple logistic regression and technology to predict landslide hazard in northeast Kansas, USA. *Engineering geology*, 69: 331-343.
- Pohl, C., J.I. Van Genderen, 1998. Multisensor image fusion in remote sensing: concepts, methods and applications. *International journal of remote sensing*, 19: 823-854.
- Tsai, T.L., J.C. Yang, 2006. Modeling of rainfall-triggered shallow landslide. *Environmental Geology*, 50: 525-534.
- Van Westen, C.J., A.C. Seijmonsbergen, F. Mantovani, 1999. Comparing landslide hazard maps. *Natural Hazards*, 20: 137-158.
- Van Western, C.J., R. Soeters, K. Sijmons, 2000. Digital geomorphological landslide hazard mapping of the Alpage area, Italy. *International journal of applied earth observation and geoinformation*, 2(1): 51-60.
- Yalcin, A., 2008. GIS-based landslide susceptibility mapping using analytical hierarchy process and bivariate statistics in ardesen (Turkey): Comparisons of results and confirmations. *Catena*, 72: 1-12.

Zolfaghari, A., A.C. Heath, 2008. A GIS application for assessing landslide hazard over a large area. *Computers and Geotechnics*, 35: 278-285.